Electronic Supplementary Material (ESI) for Physical Chemistry Chemical Physics.

Lattice oxygen activation in disordered rocksalts for boosting oxygen evolution

Menghan Zhao, Xuerong Zheng, Chengchi Cao, Qi Lu, Jinfeng Zhang, Haozhi Wang*, Zhong Huang*, Yanhui Cao, Yang Wang, Yida Deng*

M. Zhao, Q. Lu, Y. Cao, Dr. J. Zhang, Prof. X. Zheng, Prof. Y. Deng

School of Materials Science and Engineering, Tianjin Key Laboratory of Composite and Functional Materials, and Key Laboratory of Advanced Ceramics and Machining Technology of Ministry of Education, Tianjin University, Tianjin 300072, P. R. China

C. Cao, Dr. H. Wang, Dr. Z. Huang, Dr. Y. Wang, Prof. X. Zheng, Prof. Y. Deng

State Key Laboratory of Marine Resource Utilization in South China Sea, School of Materials Science and Engineering, Hainan University, Haikou 570228, P. R. China.

Experiments.

Synthesis of disordered rocksalts: The cation-disordered rock salt sample ($Li_{1.2}Fe_{0.4}Ti_{0.5}O_2$) was synthesized by high-energy ball milling. The stoichiometric amounts of FeO, TiO_2, and 5% excess Li_2O as precursors were added into 50 mL ball mill tanks containing ZrO_2 balls of 10 mm and 6 mm in diameter. The ball mill tank was mounted on a planetary ball mill running at 360 rpm for 4,000 mins for mechanical alloying. The machine rested 5 mins in every 30 mins, and the effective working time is about 55.5 hours.

Materials characterization: XRD patterns of samples was analyzed via a Bruker D8 Advanced diffractometer(Cu Kα, 40 kV, 40 mA). The morphology and composition of the products were characterized using a scanning electron microscope (SEM; JSM-7800F) equipped with energy dispersive X-ray spectroscopy (EDX). Transmission electron microscopy (TEM) was carried out on a JEOL JEM-ARM200F instrument. Raman spectra was acquired on a HORIBA Lab RAM HR Evolution (excitation wavelength of 532 nm).

Electrochemical Measurements: The ink was prepared by dispersing 10 mg of oxide catalyst in a mixture of 35 μL Nafion (5%) solution, 265 μL deionized water and 700 μL isopropanol and sonicating for one hour. The ink was droped on nickel foams with a mass loading of 0.3 mg cm^{-2} to prepare an area of 1 cm * 1 cm working electrode. To measure the catalytic activity of the catalyst for OER reaction, electrochemical tests were all performed on CHI 660E by using a standard three-electrode system. The reference electrode used during the tests was a saturated calomel electrode (SCE) and the counter electrode was a graphite electrode. The electrolyte was iron-free 1 M KOH prepared by deionized water. The scan rates for linear sweep voltammetry (LSV) tests were all 10 mV / s. The scanning voltage range of LSV is 0-0.9V vs. SCE, and the scanning process is from high potential to low potential. The electrochemical impedance spectroscopy (EIS) measurements were carried out from 10 kHz to 0.01 Hz at an potential of 0.5 V vs. SCE. All the LSV polarization curves have been 100% iR-corrected.

The turnover frequency (TOF) represents the number of oxygen molecules produced by the catalyst at the active site per unit time and can be used to reflect the catalytic kinetics of the material. The formula for calculating TOF is as follows:

$$\mathrm{TOF} = \frac{j \times A}{n \times F \times m}$$

Where A is the geometric area of the working electrode. *j* is the the current density of LSV. n is the number of electrons transferred from the reaction (for OER, n is 4). F is the Faraday constant (96500 C/mol). m is the number of moles of the catalytically active substance on the electrode.

We utilize the electrochemical double-layer capacitance (C_{dl}) to evaluate the electrochemical active surface area (ECSA). The C_{dl} was measured by cyclic voltammograms (CV) in the non-Faraday voltage range of -0.1 V to 0 V vs. SCE with the scan rate from 20 mV s^{-1} to 100 mV s^{-1}. The C_{dl} is measured by plotting the $\Delta j/2$ at -0.05 V vs. SCE against the scan rates, and the slope is C_{dl}. The formula for calculating ECSA is as follows:

$$\mathrm{ECSA} = C_{dl} / C_S$$

Where C_S is the specific capacitance for electrode with the smooth planar surface. In this work, we assumed that the specifific capacitanc of the catalysts is 60 μF cm^{-2}. The formula for calculating ECSA current density (j_{ECSA}) is as follows:

$$j_{ECSA} = A \times j / \mathrm{ECSA}$$

Where A is the geometric area of the working electrode. *j* is the the current density of LSV.

Theoretical Calculation Details: All the calculations was performed within the framework of the density functional theory (DFT) as implemented in the Vienna Ab initio Software Package (VASP 5.4.4) code within the Perdew–Burke–Ernzerhof (PBE) generalized gradient approximation and the projected augmented wave (PAW) method.

The cutoff energy for the plane-wave basis set was set to 400 eV. The Brillouin zone of the surface unit cell was sampled by Monkhorst–Pack (MP) grids, with a k-point mesh for DRX and $LiFePO_4$ structure optimizations. The DRX and $LiFePO_4$ surfaces were determined by 3 × 3 × 1 Monkhorst−Pack grid. The convergence criterion for the electronic self-consistent iteration and force was set to 10^{-5} eV and 0.01 eV/Å, respectively. The PBE+U approach was applied to calculations of the electronic structure of DRX and $LiFePO_4$ which can partly reduce the underestimation of the electronic band gap and the excessive tendency to delocalize the electron density. In this work, we set the Hubbard parameter to U − J = 3 and 4 eV for Ti and Fe, which ensures a good qualitative description of structure and electronic properties of Ti and Fe oxide. A vacuum layer of 15 Å was introduced to avoid interactions between periodic images.

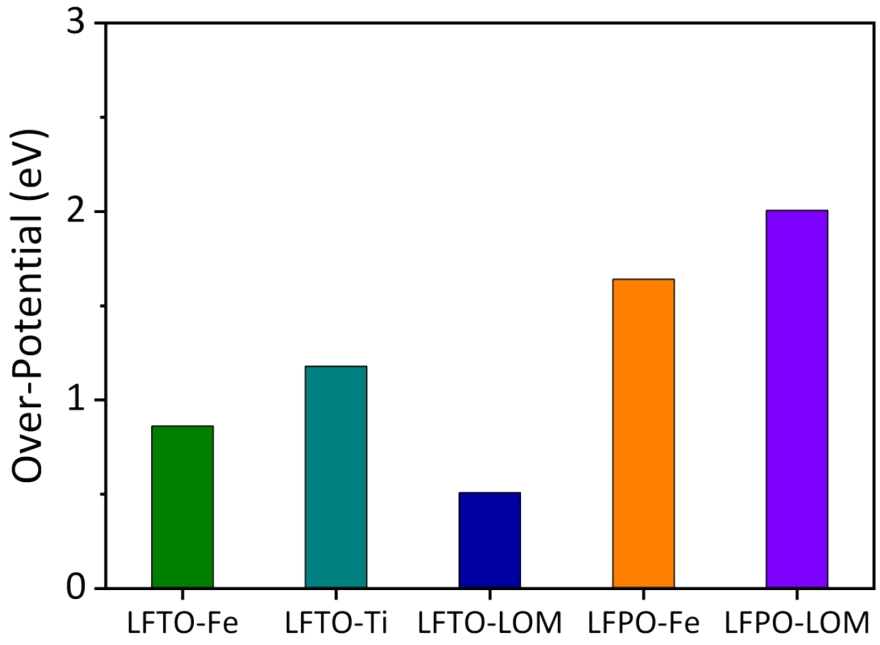

Figure S1. Comparison of rate-limiting step Gibbs free energy difference of samples in different OER mechanism.

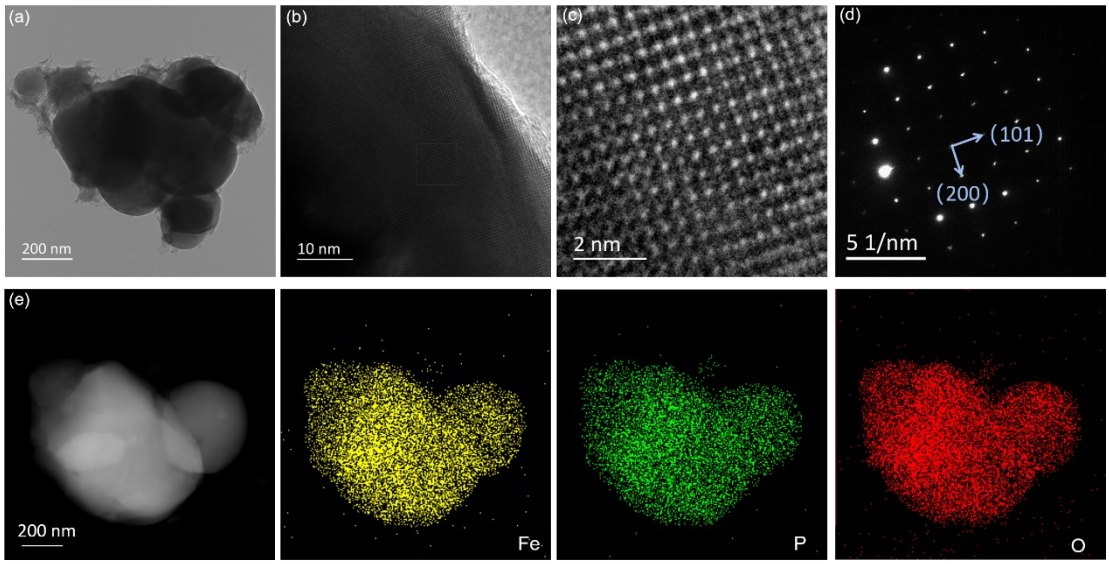

Figure S2. Morphological characterizations of $LiFePO_4$. (a-c)TEM and HRTEM images of LiFePO4; (d) The electron diffraction spots of $LiFePO_4$; (e) HADDF-STEM and EDS mapping of elemental distribution in a particle of $LiFePO_4$.

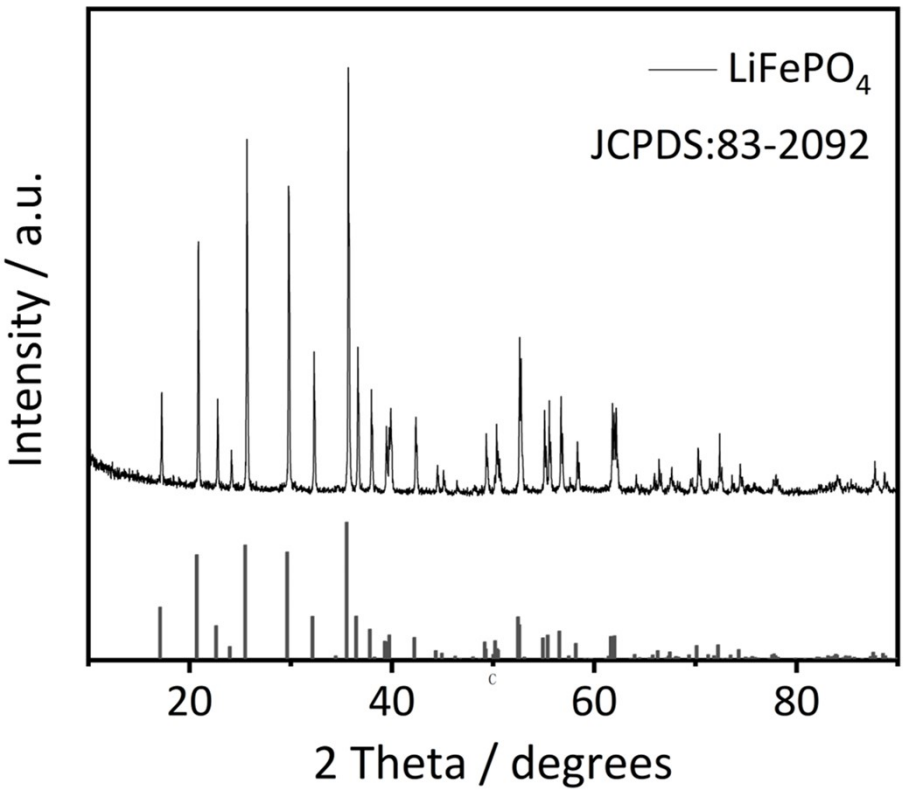

Figure S3. Phase characterization of $LiFePO_4$. XRD patterns of $LiFePO_4$.

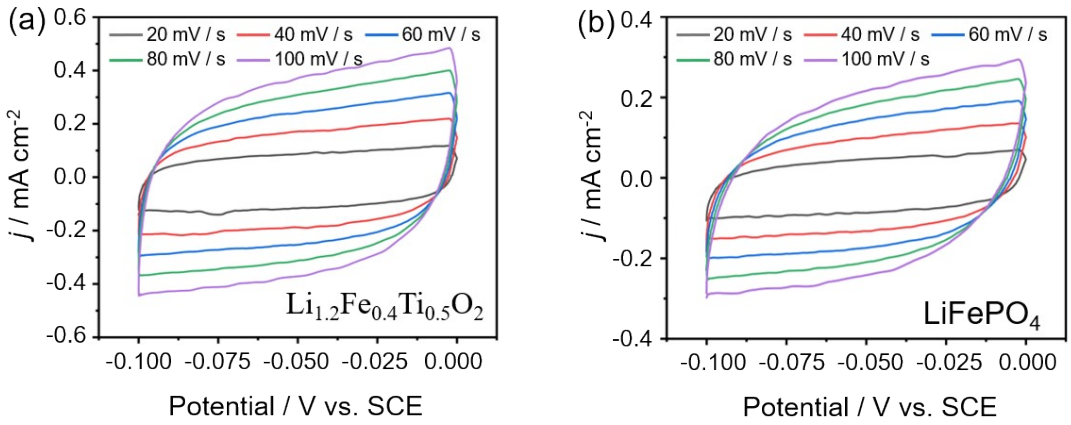

Figure S4. CV diagrams of $Li_{1.2}Fe_{0.4}Ti_{0.5}O_2$ and $LiFePO_4$ at non-Faradaic region.

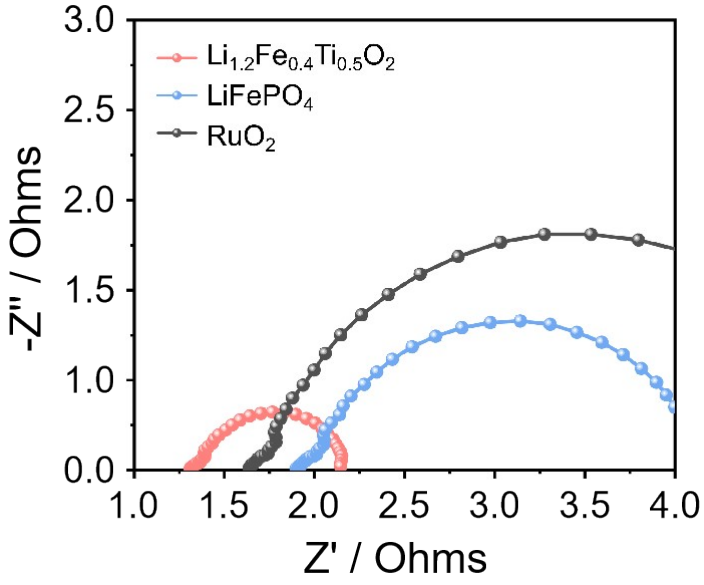

Figure S5. The EIS results of $Li_{1.2}Fe_{0.4}Ti_{0.5}O_2$, $LiFePO_4$, and RuO_2.

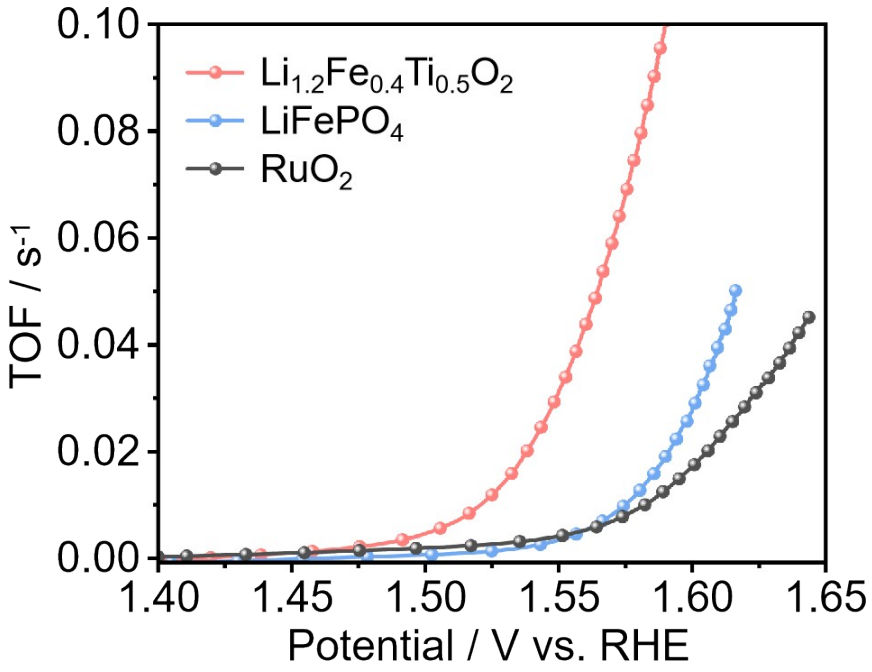

Figure S6. Curves of TOF of $Li_{1.2}Fe_{0.4}Ti_{0.5}O_2$, $LiFePO_4$ and RuO_2.

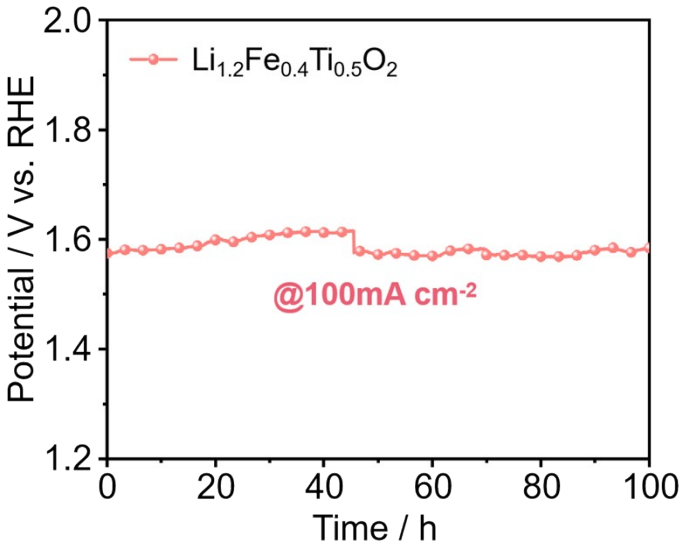

Figure S7. The chronopotentiometry response of $Li_{1.2}Fe_{0.4}Ti_{0.5}O_2$ at 100 mA cm^{-2}.

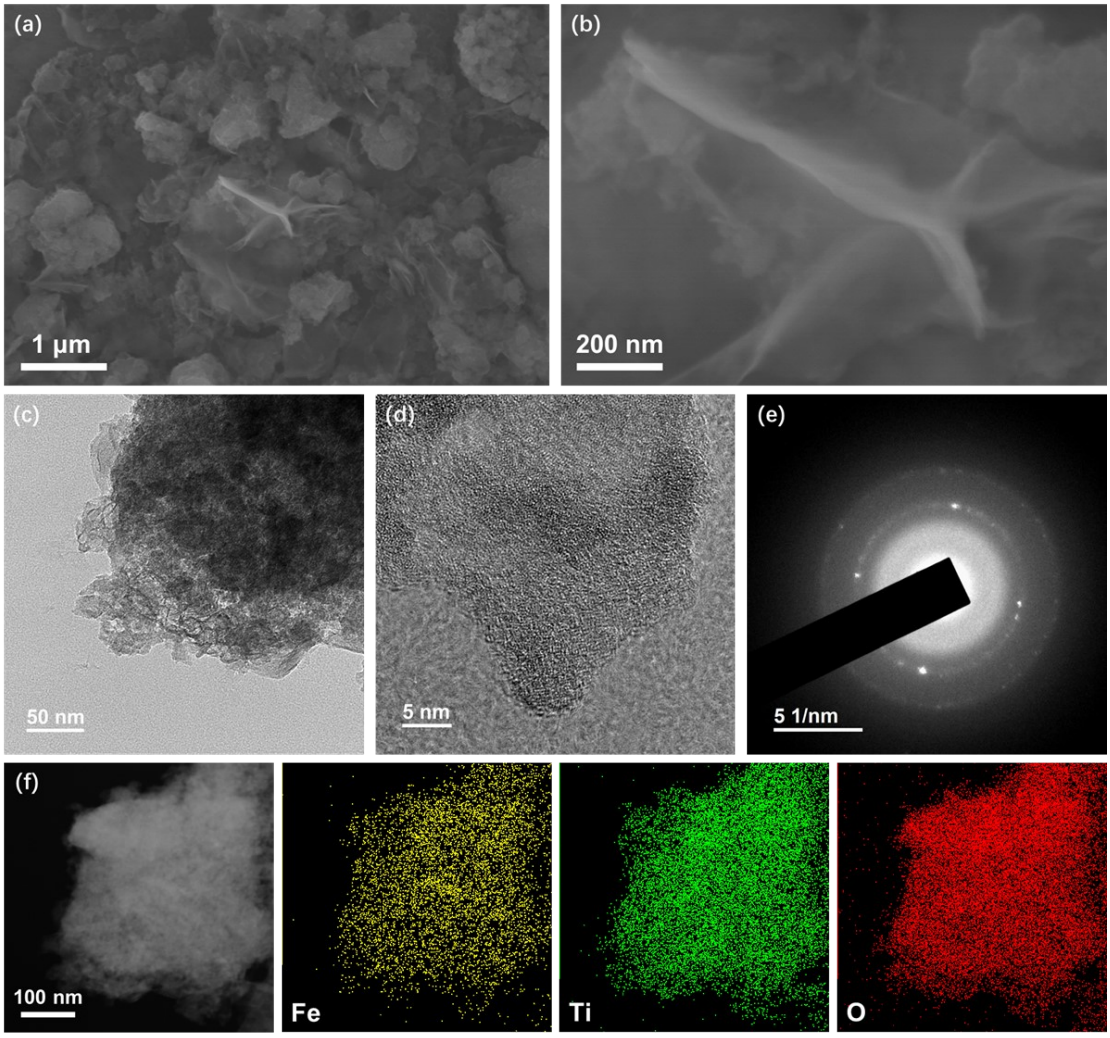

Figure S8. Morphological characterizations of $Li_{1.2}Fe_{0.4}Ti_{0.5}O_2$ after 100 hours OER reaction at the current density of 10 mA cm^{-2}; (a-b) SEM images; (c-d) TEM and HRTEM images; (e) FFT diffraction rings; (d) HADDF-STEM and elemental mapping images of $Li_{1.2}Fe_{0.4}Ti_{0.5}O_2$ after OER.

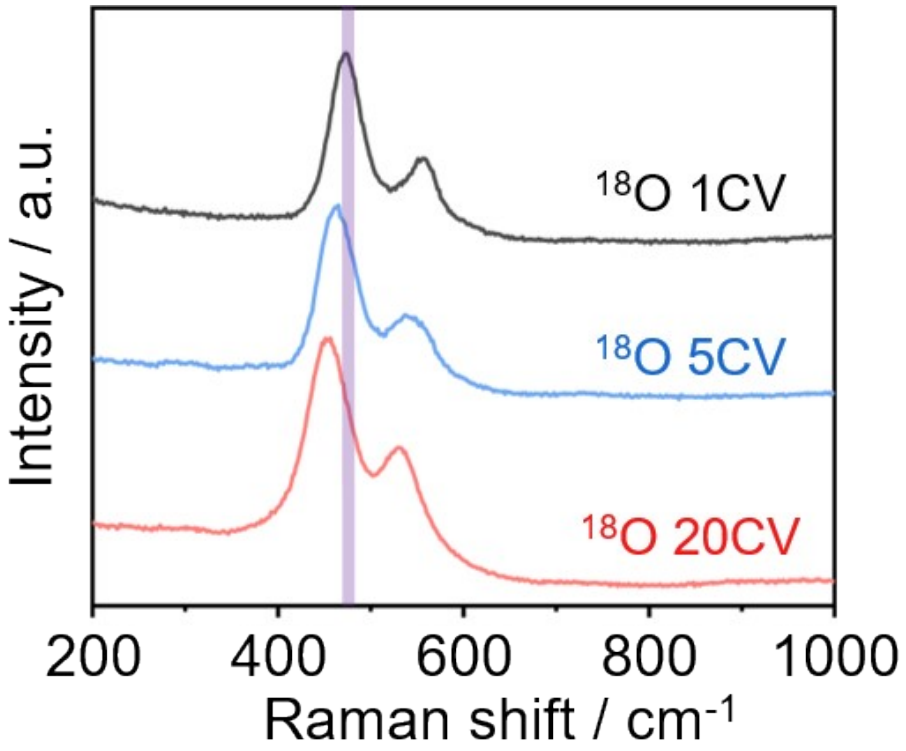

Figure S9. Raman spectra of $Li_{1.2}Fe_{0.4}Ti_{0.5}O_2$ by CV processing in the ^{18}O labeled KOH.

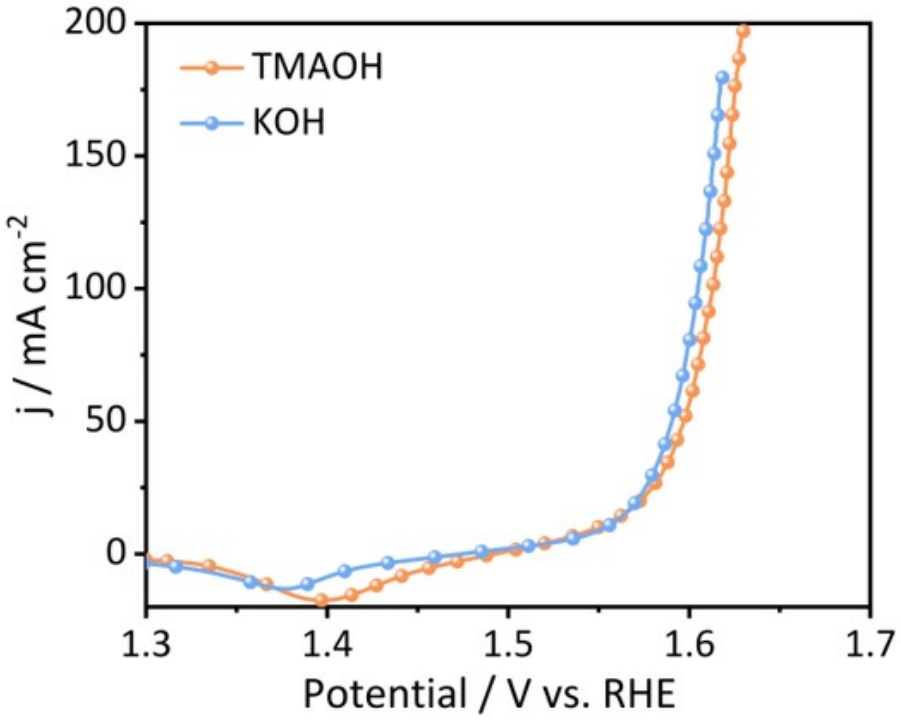

Figure S10. OER LSV curves of $LiFePO_4$ in 1 M KOH and 1 M TMAOH solution.